Supporting Information

Two-dimensional $Ti_3C_2T_X$ MXene@TiO_2/MoS_2 heterostructure with excellent selectivity for the room temperature detection of ammonia

Xu Tian [a], Lijia Yao [a], Xiuxiu Cui [a], Rongjun Zhao [a], Ting Chen [b*], Xuechun Xiao [c*], Yude Wang [d*]

a *School of Materials and Energy, Yunnan University, 6500504 Kunming, People's Republic of China*

b *Institute of Materials Science & Devices, School of Materials Science and Engineering, Suzhou University of Science and Technology, Suzhou, 215009, People's Republic of China.*

c *Key Lab of Quantum Information of Yunnan Province, Yunnan University, 6500504 Kunming, People's Republic of China.*

d *Yunnan Key Laboratory of Carbon Neutrality and Green Low-carbon Technologies, Yunnan University, 650504 Kunming, People's Republic of China.*

* To whom correspondence should be addressed. E-mail: chenting@mail.usts.edu.cn (T. Chen), xchxiao@ynu.edu.cn (X. C. Xiao), ydwang@ynu.edu.cn (Y. D. Wang)

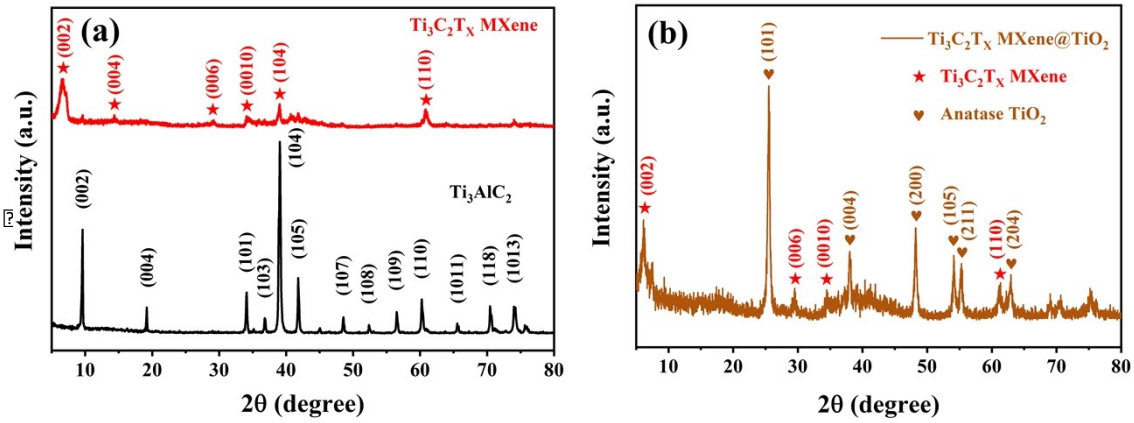

Fig. S1. XRD patterns of (a) Ti_3AlC_2 and $Ti_3C_2T_X$ MXene, (b) $Ti_3C_2T_X$ MXene@TiO_2.

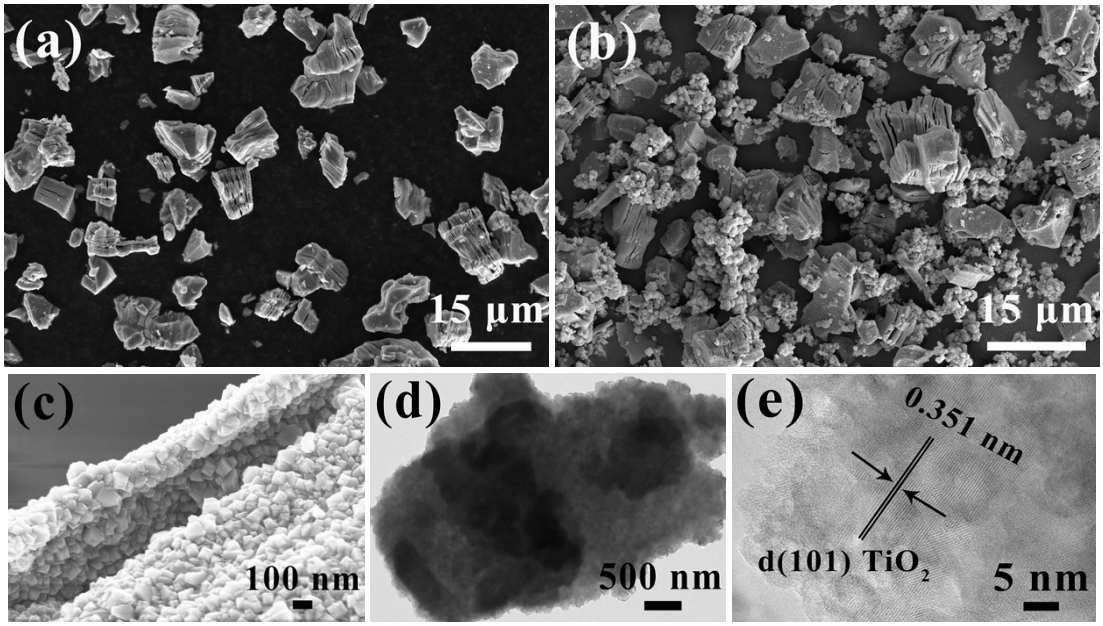

Fig. S2. Low magnification SEM images of (a) $Ti_3C_2T_X$ MXene powder, (b) $Ti_3C_2T_X$ MXene@TiO_2/MoS_2 nanocomposite, (c) $Ti_3C_2T_X$ MXene@TiO_2.

TEM image: (d) $Ti_3C_2T_X$ MXene@TiO_2, HRTEM image: (e) $Ti_3C_2T_X$ MXene@TiO_2.

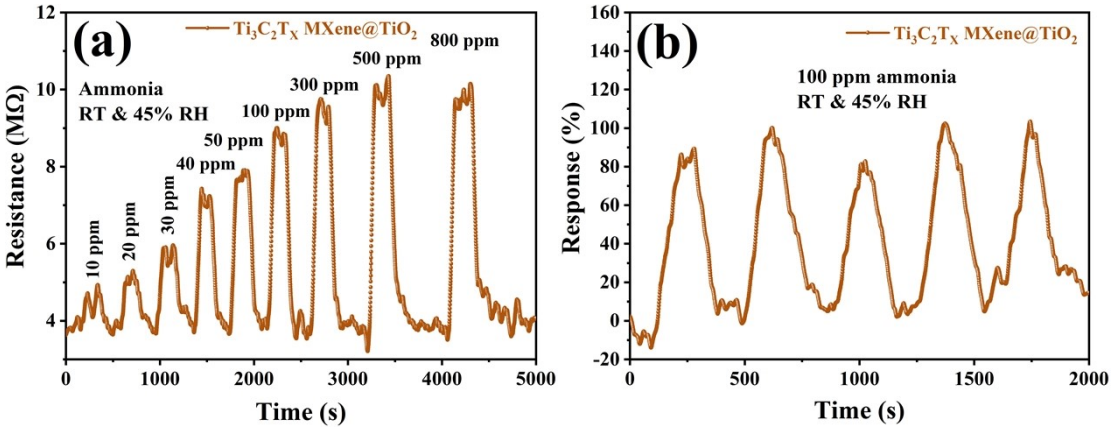

Fig. S3. (a) Resistance of $Ti_3C_2T_X$ MXene@TiO_2 sensor to different concentration of ammonia vapor; (b) The reproducibility of the $Ti_3C_2T_X$ MXene@TiO_2 sensor to 100 ppm ammonia at RT of 26 ^oC and RH of 46%.

Computational method

We have employed the Vienna Ab Initio Package (VASP) to perform all the density functional theory (DFT) calculations within the generalized gradient approximation (GGA) using the PBE formulation. We have chosen the projected augmented wave (PAW) potentials to describe the ionic cores and take valence electrons into account using a plane wave basis set with a kinetic energy cutoff of 400 eV. Partial occupancies of the Kohn−Sham orbitals were allowed using the Gaussian smearing method and a width of 0.05 eV. The electronic energy was considered self-consistent when the energy change was smaller than 10-5 eV. A geometry optimization was considered convergent when the force change was smaller than 0.02 eV/Å. Grimme's DFT-D3 methodology was used to describe the dispersion interactions.

The equilibrium lattice constant of hexagonal MoS_2 (002) monolayer unit cell separated by a vacuum layer in the depth of 15 Å was optimized, when using a 15×15×1 Monkhorst-Pack k-point grid for Brillouin zone sampling, to be a=3.165 Å. And that of hexagonal $Ti_3C_2F_2$ (002) monolayer unit cell was optimized to be 3.060 Å. We then use the two to construct a MoS_2 (002)/ $Ti_3C_2F_2$ (002) heterojunction model with p(4x4) periodicity in the x and y directions and a vacuum layer in the depth of 15 Å in order to separate the surface slab from its periodic duplicates. This model comprises of 16 Mo, 32 S, 48 Ti, 32 C and 32 F atoms. During structural optimizations, the gamma point in the Brillouin zone was used for k-point sampling, and all atoms were allowed to relax.

The adsorption energy (Eads) of adsorbate A was defined as:

$$E_{ads} = E_{A/surf} - E_{surf} - E_{A(g)}$$

where $E_{A/surf}$, E_{surf} and $E_{A(g)}$ are the energy of adsorbate A adsorbed on the surface, the energy of clean surface, and the energy of isolated A molecule in a cubic periodic box with a side length of 20 Å and a 1×1×1 Monkhorst-Pack k-point grid for Brillouin zone sampling, respectively.